Iranian Polymer Journal (2021) 30:547–557
https://doi.org/10.1007/s13726-021-00911-2

ORIGINAL RESEARCH

The effect of epoxidized vegetable oil and phthalic anhydride as compatibilizers on properties of rubber seed shell/polypropylene composites

Mohamad Danial Shafiq[1] · **Hanafi Ismail**[1]

Received: 26 August 2020 / Accepted: 4 March 2021 / Published online: 12 March 2021

Abstract
Numerous adverse effects are reported from excessive usage of synthetic polyolefins including major environmental concerns. Since then, the development of natural-based polymer composites is escalating, to replace the versatile conventional plastics that possess excellent mechanical and thermal properties. Rubber seed shell (RSS) is a novel and abundant natural-based substituent that is highly composed of hemicellulose and cellulose. In this work, we reported on the performance of RSS-filled polypropylene composites added with two different types of compatibilizers: epoxidized vegetable oil (EVO) and phthalic anhydride (PA). The composites were produced using a Haake internal mixer and a compression molding. The tensile, flexural, and impact properties of the composites were analyzed. Later, we investigated the thermal stability and water absorptivity of the composites. The mechanical, thermal, and water absorption properties of the RSS-filled composites deteriorated with increasing RSS loadings. For both EVO and PA-compatibilized systems, the mechanical properties were enhanced except for the elongation-at-break of the composites. PA-compatibilized composites recorded better thermal stability and water absorption resistance under ambient conditions compared to RSS composites with EVO. The qualitative structural evidence of the composites enhanced properties and deterioration were observed using a Zeiss Supra scanning electron microscope. As a novel natural filler, RSS has adequately proven its practicability in manufacturing environmentally friendly natural composites with acceptable mechanical and thermal properties.

Keyword Natural filler · Polymer composite · Rubber seed shell · Mechanical properties · Thermal properties

Introduction

Immense technological advancement in recent decades concerns the environment. This includes plastic wastes pollution and management, which threatens the environment. The overall process of plastic waste management which comprises collecting, sorting, washing, sizing, and reclaiming the plastic wastes, can be costly and require high energy consumption and dissipation [1–3]. Plastic waste incineration is another approach to control plastic waste issues which are very useful for energy generation. However, the energy regeneration process requires thorough pre-processes such as the aforementioned plastic waste management approach, which in turn requires more energy to regenerate energy from waste plastics. Since then, the production of degradable plastics has garnered attention among scientists as one of the ways to solve plastic waste issues. In the production of biodegradable plastic-based products, starch is normally incorporated up to 50% to replace the synthetic polymer. Plastic wastes turn into carbon dioxide and water through depolymerization and mineralization after being exposed to natural environments such as weathering and soil burial [4]. Due to the increasing demand for (bio)degradable plastics, the production cost can be twice as much compared to conventional plastic at present [5]. Starches are widely used in an extensive range of food for multiple purposes including stability modifier, as a thickening and gelling agent due to its versatility to serve as a principal food reserve and it also contains nutritional values for the human diet [6]. In underdeveloped countries, starches serve the nation as their main

✉ Mohamad Danial Shafiq
danialshafiq@usm.my

[1] School of Materials and Mineral Resources Engineering, Universiti Sains Malaysia, Engineering Campus, 14300 Nibong Tebal, Penang, Malaysia

source of diet due to the abundant source of starch-based plants such as cassava and sweet potato [7].

In recent decades, researchers have competitively investigated the production and properties of natural filler-based polymer composites due to the abundance, lightweight, low processing cost, tolerable mechanical properties, and degradability of natural fillers [8, 9]. The compositions of natural fillers include lignin and celluloses, which impart an inferior load-bearing capability of the end composites compared to synthetic-filled polymers. The range of applicability of polymer-based composites is gauged between superior mechanical properties, which is often observed in synthetic-filled composites such as carbon and glass fibers, and the sustainability and degradability of composites, depending on the life span of certain products. The annual demand for natural fibers is growing to 15–20% with major applications in packaging and automotive [10, 11]. Extensive research on composites made of natural renewable sources has increased the potential to produce cost-effective, non-hazardous, and sustainable polymer composites with moderate mechanical properties mainly for packaging and automotive applications, hence substituting the need for petroleum-based polymers and food-based materials.

Rubber seed is an agricultural by-product of the rubber tree. Rubber seed is lightweight, ovoid, and flattened on one side, consists of a hard and brittle shell loosely containing a cream-colored kernel [12]. The rubber seed shell (RSS) is composed of similar substituents in other natural fillers such as kenaf, sisal, hemp, and jute with the amount of ash in RSS is 0.82%, lignin 2.98%, hemicellulose 24.56%, and the largest composition is cellulose (71.64%) [13, 14]. Malaysia is one of few countries with large rubber plantations hence enabling us to utilize the RSS, which were previously neglected as natural waste, despite their versatility as a natural filler in polymer composites. The composition of conventional natural fillers such as kenaf and jute can produce polymer composites with tailorable mechanical and thermal properties as well as ensuring products' sustainability provide us with options to produce natural-based polymer composites using RSS [15, 16].

The advantages promoted by natural fillers in polymer matrix composites have some major drawbacks. The incorporation of natural fillers in polymers observed certain degrees of compensation in mechanical properties such as tensile, flexural, and impact properties of the composites. Poor matrix–fiber interactions and water resistance results in a loss in the end properties of the composites and obstructs their applicability in industries. Several strategies have been practiced promoting the deficiency in matrix-filler compatibility including the utilization of coupling agents, compatibilizers, surface treatment, and modifications. In this work, we utilize the abundant RSS as a novel natural filler in polyolefin and incorporate two different classes of compatibilizers to tailor the properties spectrum of RSS-filled polymer composites.

Experimental

Materials

Polypropylene (PP) pellets grade Propelinas 200D was acquired from Titan Malaysia Sdn. Bhd. Rubber seed shells (RSS) were collected from several rubber plantations in Kelantan and Pahang, Malaysia. Epoxidized vegetable oil (EVO) was synthesized by Tan et al. [17]. Phthalic anhydride (PA) was acquired from Sigma-Aldrich, Malaysia.

Methods

The rubber seed shells (RSS) were separated from their kernel and dried in an oven for 1 h at 100 °C before being ground into flour using a high-speed grinding machine. Then, the ground RSS was sieved and their particle size was measured using a Malvern Mastersizer, confirming the average particle size of 100 µm. PP and RSS were mixed in a Haake Rheomix mixer Model R600/610 at 160 °C with a rotating torque of 50 rpm for 10 min. RSS loadings were varied from 0, 10, 20, 30 and 40 php. Epoxidized vegetable oil and phthalic anhydride were added in a separate series at 3 php each for all RSS loadings. PP/RSS composites and EVO, PA-compatibilized PP/RSS composites were compression-molded using an electrical heated hydraulic press compression machine. The heat press process started with a preheating at 150 °C for 6 min, followed by compression with a pressure of 1000 kg/m^3 for 4 min at the same temperature. All compression molded sheets (150 mm × 150 mm × 1 mm) were cold-pressed for 2 min.

Mechanical testing

Tensile properties were determined in accordance with ASTM D638 using a Testometric tensometer M500 with a gauge of crosshead speed of 5 mm/min. Flexural properties were examined based on ASTM D790-92 (three-point bending) and an unnotched Izod impact test was carried out based on ASTM D256 using a Zwick impact-testing model 5101.

Surface morphology

Tensile surface fracture of the composites was qualitatively observed using a Zeiss Supra 35 VP, operated at 10 kV accelerating voltage. The samples were prepared using a Polaron SC 515 sputter coater.

Water absorption and thermal properties

The water absorption test for the composites was performed based on ASTM D570 at ambient conditions. The percentage of water absorption was calculated using Eq. (1) that M_1 and M_0 were the final mass of the composites after immersion and the initial mass of the composites before immersion. The thermal stability of the composites was analyzed using a Q500 Perkin-Elmer Instrument at a heating rate of 20 °C/min, from room temperature, up to 800 °C under a nitrogen atmosphere of 50 mL/min.

$$\text{Water absorption } (\%) = \frac{(M_1 - M_0)}{M_0} \times 100\% \quad (1)$$

Results and discussion

The effect of EVO and PA on the mechanical properties of PP/RSS composites

The addition of rubber seed shell (RSS) in polypropylene (PP) has significantly reduced the tensile strength, σ_s, of the composites by 60% of the σ_s of neat PP, at only 10 php of RSS. Figures 1, 2 and 3 show the tensile properties; tensile strength (σ_s), elongation-at-break (EB) and Young's modulus (E_Y) of uncompatibilized and compatibilized PP/RSS composites, respectively. From Fig. 1, the trend was seen to decline consistently with increasing RSS loading at up to 40 php. Epoxidized vegetable oil (EVO) and phthalic anhydride were proven to improve the σ_s of PP/RSS composites and the trend was steadily observed for composites with all RSS loadings. It was revealed that RSS has a large particle size with irregular geometries as reported by Shafiq et al. [18]. This justifies the σ_s reduction of PP/RSS composites with increasing RSS loading. At 40 php RSS loading, where the σ_s of the composite was the least, is hugely contributed to a higher tendency of RSS particles forming inter-filler interactions compared to low RSS loadings. This can be evidently confirmed by the trend variation of the elongation-at-break (Fig. 2) and Young's modulus (Fig. 3) of neat PP and PP/RSS composites. The rigidity enhancement is commonly observed in filled-polymer composites [19].

Crack initiation and propagation mechanisms can be ruled in for the failure of composite materials [20]. The

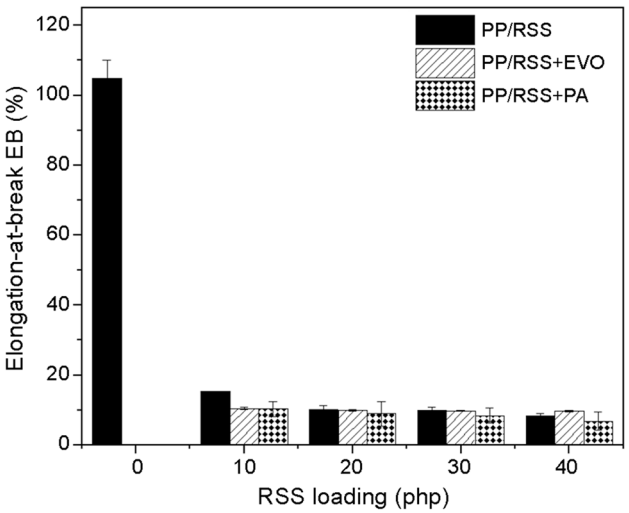

Fig. 2 Elongation-at-break (EB) of PP/RSS composites without/with EVO or PA

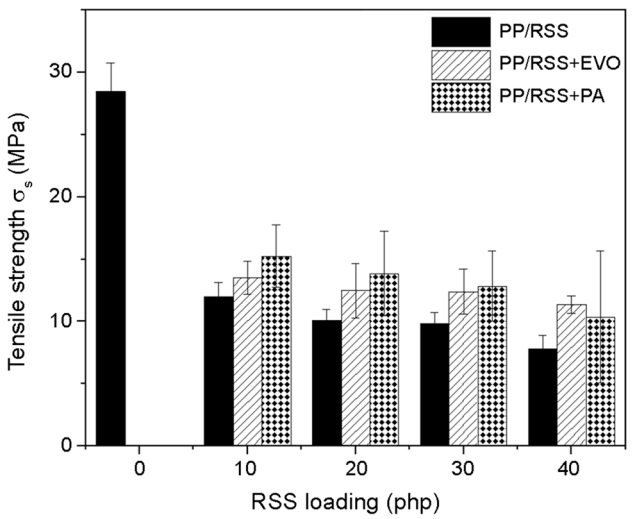

Fig. 1 Tensile strength (σ_s) of PP/RSS composites without/with EVO or PA

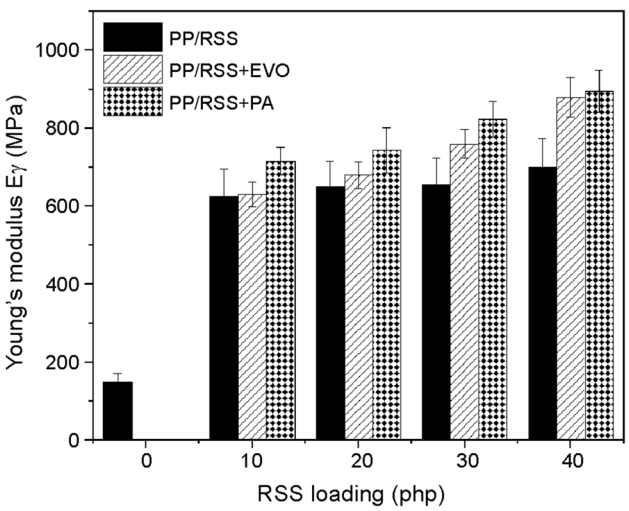

Fig. 3 Young's modulus (E_Y) of PP/RSS composites without/with EVO or PA

agglomeration of RSS fillers is prone to occur with increasing concentration of RSS, enabling the stress concentration regions in composites, which only needs a small amount of energy to fail. Highly filled composites fail in a brittle manner at a very low-stress level and elongation. The agglomeration of natural fillers is often induced by the interactions between hydrophilic sites of natural fillers such as RSS, wood-based, and starch-based fillers [18, 21]. Figure 4 shows the tensile fracture surfaces of neat PP and PP/RSS composites. At high filler loadings, the incompatibility between the polymer matrix and filler regions is more pronounced. These results in filler pull-outs when the composite is exerted with tensile force, yielding the formation of gaps and voids as depicted in Fig. 4. The tensile fracture surface micrograph for neat PP in Fig. 4a shows a ductile failure and when RSS was added to the system, more brittle fracture surfaces were observed. In Fig. 4b, the '*V*' region is identified as the formation of void on a tensile fracture surface of a composite with 20 php of RSS. Meanwhile, Fig. 4c presents the fracture surface of a composite with 40 php of RSS, where the '*B*' region indicates a bulky lump formed with an approximate size of 130 µm and region '*P*' reveals a pull-out trace with an approximate area of 0.1 mm^2. Ismail et al. revealed that ground RSS has irregular particle shapes ranging from a few to hundreds of microns, also indicating that ground RSS has multiple aspect ratios with polydispersed particles [18]. Heterogenous particle size and shape of fillers tend to form filler agglomeration and sedimentation, hence declining the mechanical properties of the composites [22, 23]. Fillers with high aspect ratios such as fibers (aspect ratio up to 200) tend to reinforce the polymer matrix by transferring the applied stress from the polymer matrix to the filler surface due to its large surface area, yielding superior mechanical properties. In contrast, spherical filler particles having symmetrical particle shape of aspect ratio equal to 1 have the minimum reinforcing ability [23].

The tensile properties of PP/RSS composites witnessed an improvement when two types of compatibilizers were added into the system. The trend was seen to be consistent for all RSS loadings except for PP/RSS of 40 php. First, the epoxidized vegetable oil (EVO) was able to improve the σ_s of PP composites up to 40% when RSS was added up to 40 php. The E_Y of PP composites also showed an increasing trend when the system was added with EVO. The hydrocarbon chain in EVO can intertwine with PP, thus forming an enforced intermolecular network or chemical cross-linking. Figure 5a, b compare the tensile fracture surface of PP/RSS composites with EVO at 20 php and 40 php of RSS. EVO-compatibilized RSS composites revealed smoother fracture surfaces, especially at 20 php of RSS, both polymer and filler were observed compatible and homogenous. At 40 php of RSS, several voids were observed although the micrograph revealed a fracture

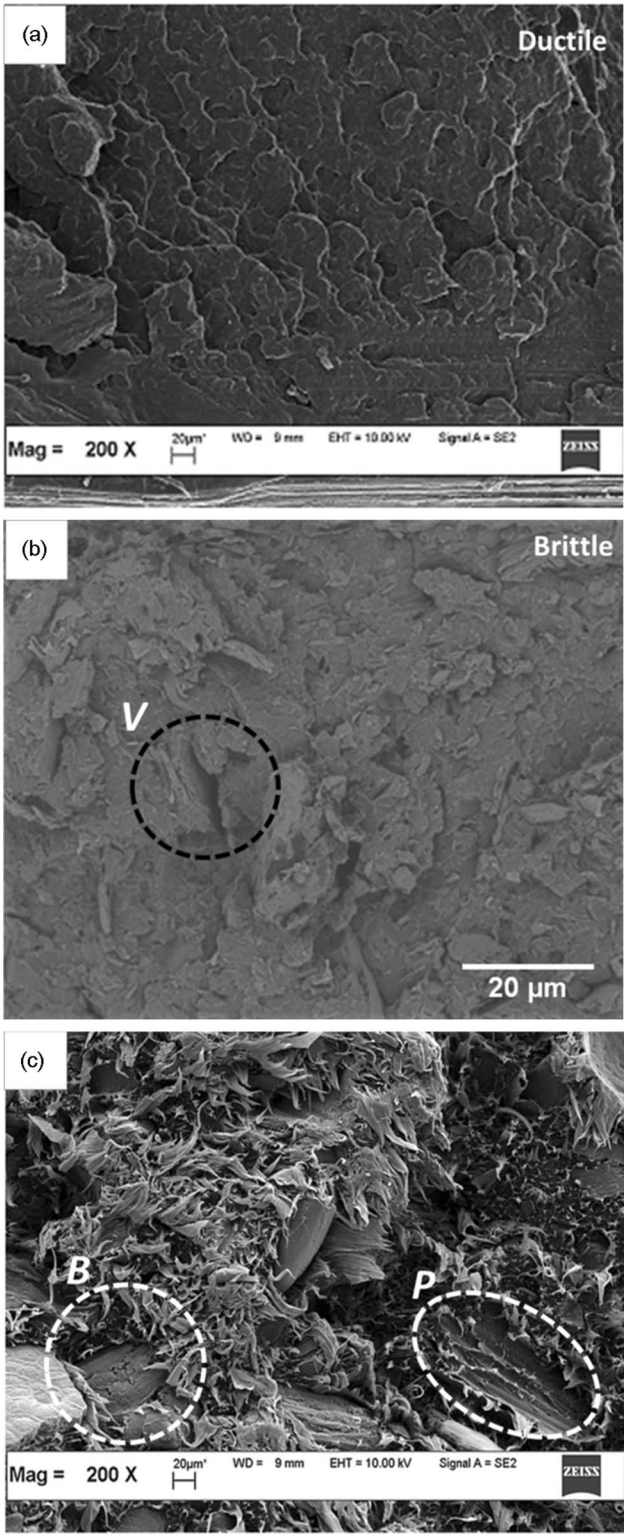

Fig. 4 Tensile fracture surface micrographs of PP/RSS composites: **a** without RSS, **b** with 20 php of RSS, and **c** 40 php of RSS at 200 × magnification

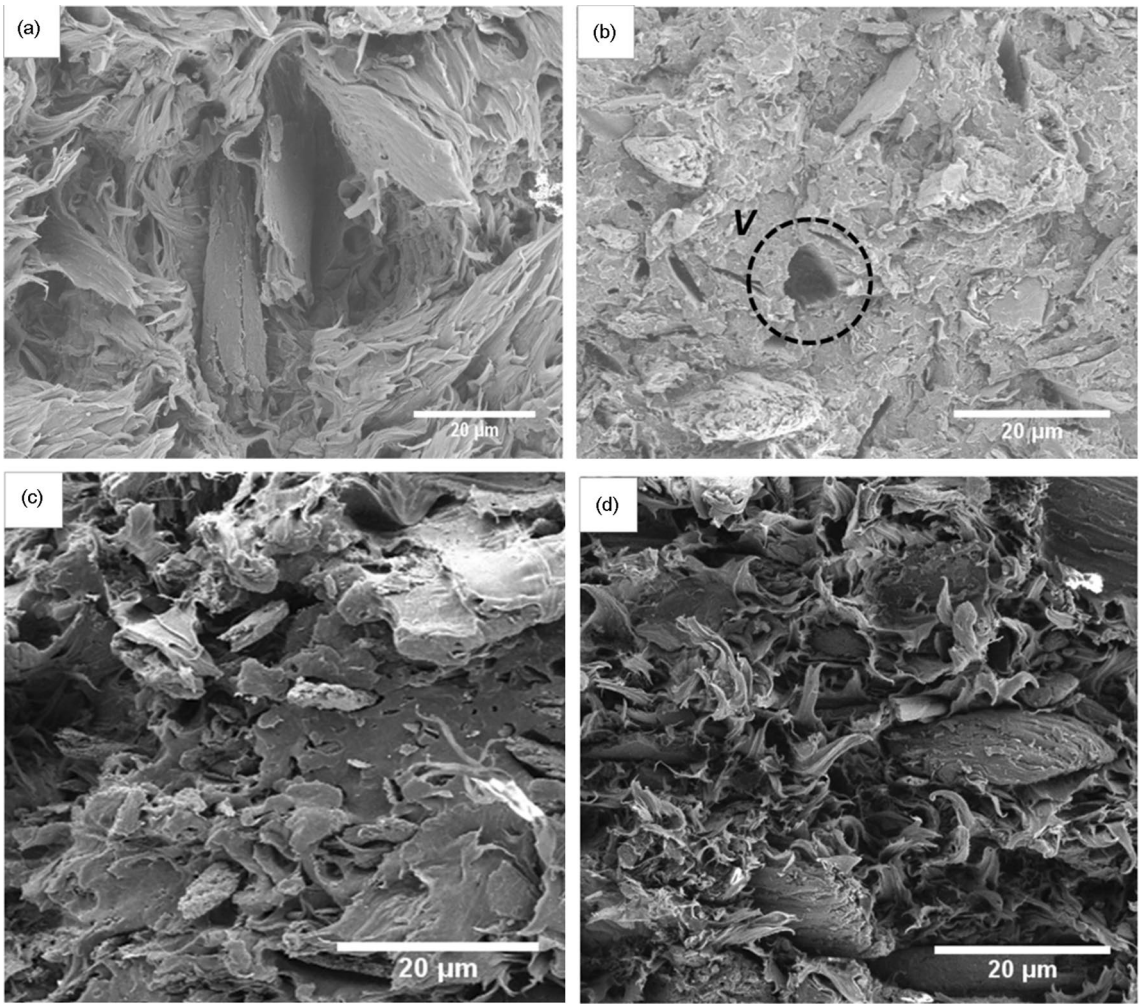

Fig. 5 Tensile fracture surface micrographs of PP/RSS composites with: **a** 20 php of RSS + EVO, **b** 40 php pf RSS + EVO, **c** 20 php of RSS + PA, and **d** 40 php of RSS + PA at 200 × magnification

surface homogeneity. The enhancement in mechanical properties of PP/RSS composites was not just observed in its tensile properties but also in the flexural, σ_f, and impact strengths, σ_I, and flexural modulus, E_f. Figures 6, 7 and 8 show the flexural strength, flexural modulus and impact strength of PP/RSS composites with/without PA and EVO, respectively. This is predominantly caused by the improvement in interfacial bonding between PP and RSS, aided by the presence of epoxy reactive sites that form chemical secondary bonding between PP and RSS. The ability of EVO to improve the overall mechanical properties of RSS-filled composites weakens its *EB* value. The stiffness of the carbon–carbon double bond in fatty acids of EVO hinders the elongation and mobility of the composite. Silverajah et al. [24] observed a similar trend in modified poly(lactic acid) (PLA) composites with epoxidized palm oil (EPO). The vegetable oil is dispersed in the polymer matrix interface, efficiently reducing the stress concentration points

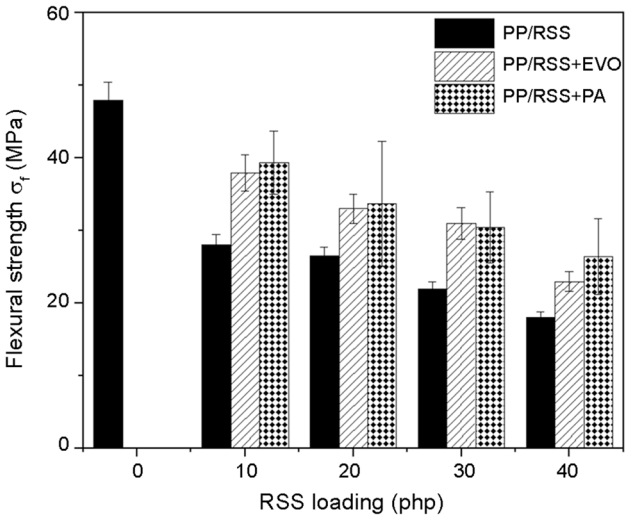

Fig. 6 Flexural strength, σ_f, of PP/RSS composites without/with EVO or PA

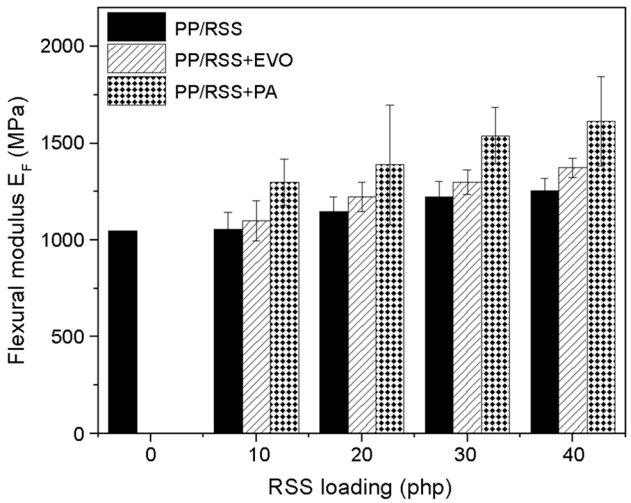

Fig. 7 Flexural modulus, E_f, of PP/RSS composites without/with EVO or PA

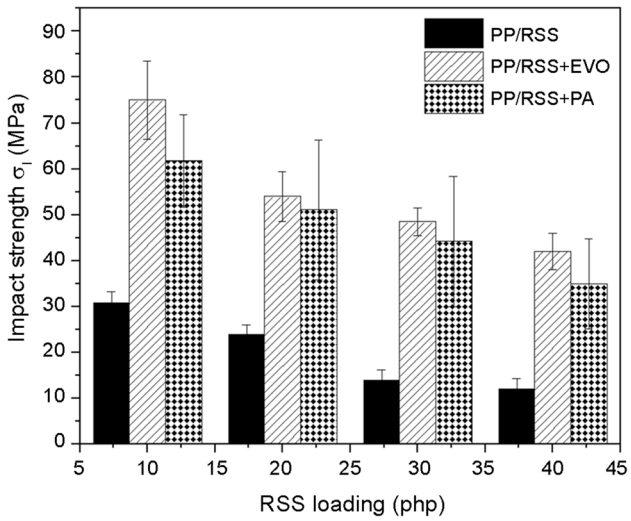

Fig. 8 Impact strength, σ_I, of PP/RSS composites without/with EVO or PA

throughout the composites, thus producing composites with enhanced mechanical strength [25, 26].

Figure 8 compares the impact strength, σ_I, of PP/RSS composites with/without EVO at increasing RSS concentration. Virgin PP sample recorded no unnotched impact strength value due to its ductility and σ_I of the filled PP composites decreases with RSS concentrations. High natural filler content in polymer composites induces a large proportion of disparity between the matrix and filler, which resulted in filler agglomerations due to strong inter-fillers interactions. The σ_I for EVO-compatibilized PP/RSS composites was enhanced by more than 100% for all RSS concentrations, with the highest being 75 J/m at 10 php of RSS and 42 J/m at 40 php of RSS for EVO-compatibilized composites. Silverajah et al. [24] explained that vegetable-based oil acts as a plasticizer, causing an improvement in the toughness of the composite. The unnotched impact energy can be transferred more efficiently throughout the composites system due to the progression in interfacial matrix-filler bonding by decreasing the number of localized stress concentration regions [27].

The addition of phthalic anhydride (PA) in PP/RSS composites has significantly improved σ_s and E_Y of the composites and adversely affected its elongation-at-break (EB). The stress transfer mechanism at high-stress regimes from the polymer matrix to the filler was enabled through improved interfacial matrix-filler bonding. In an anhydride-based compatibilizer, the hydrophilic hydroxide groups can easily form ester linkages with the anhydrides [28, 29]. The dramatic decrease of EB for PP/RSS composites and PA-modified PP/RSS composites are depicted in Fig. 2. Without the presence of a compatibilizer for the composites at low filler concentration, the domination of the matrix phase makes the *EB* high and the matrix becomes a dispersed phase when extended [30]. The stiffening effect that is provided by RSS filler and enhanced by the addition of PA restricts the molecules to flow past each other and elongate, hence restricting the mobility of polymer chains by decreasing the deformability of rigid interface between RSS and PP matrix. Figures 5c, d illustrate better dispersibility and homogeneity of tensile fracture surfaces for PA-compatibilized composites at 20 and 40 php of RSS. This may be related to the immense increment of E_Y of PA-compatibilized PP/RSS composites as presented in Fig. 3. Overall, the improvement in modulus of approximately 12–16% for PA-compatibilized PP/RSS composites compared to its counterpart. In another polymeric composites application, PA is widely used as a hardener in polymer-based composites due to its rigidity, crystallinity, and needle-like shape [31]. The improvement in interfacial adhesion by chemical interaction restricts the deformation capacity of the matrix in the elastic zone and increases the modulus [32]. A similar finding was reported in the previous research, incorporating Luffa fiber with PP [32]. The flexural strength and modulus depicted in Figs. 6 and 7 show a similar trend with the σ_s and E_Y of PA-compatibilized PP/RSS composites. An improvement in PP-RSS interfacial bonding hinders the formation of voids and spaces at the bending point when flexural stress is applied. The flexural stress is uniformly transferred throughout the composites structure; thus, the composite resisting to fail or failure at high applied stress.

Comparing the σ_I of PP/RSS composites with/without PA, the vast improvement of the impact strength value with enhanced by 50% is observed for all RSS loadings. However, referring to Fig. 8, the σ_I of EVO-compatibilized PP/RSS composites is higher than composites with PA at all

RSS concentrations. Impact strength implies the degree of the brittleness of the polymer and the ductility spectrum of polymers can be modified by adding additives such as oils, where oils provide a plasticizing effect in polymers [33, 34]. The ability of EVO to extend the polymer network through epoxide linkages made PP/RSS composites tougher than PA compatibilized PP/RSS composites.

The effect of EVO and PA on the thermal properties of PP/RSS composites

The thermogravimetric analysis (TGA) thermogram of PP/RSS composites with/without EVO is tabulated in Fig. 9. Neat PP sample shows a single mass loss % at 502.34 °C with a total mass loss of 99.94%. The plot shifted to 533–534 °C when RSS was added at 20 and 40 php. EVO-compatibilized composites recorded a maximum mass loss at a lower temperature of 450–465 °C. The first mass loss was recorded for RSS-filled composites with a gradual slope at 250–450 °C. This is mainly caused by the decomposition of hemicelluloses and lignin in RSSF. Despite having more lignocelluloses content, the composite with 40 php RSS degrades fully at a slightly higher temperature than PPRSS 20, yielding slightly higher residue. At a high temperature, the dissociation of carbon bond yields radicals, and the recombination of radicals that possibly occurred improved the interactions between matrix radicals and filler surface. The presence of EVO shifted the first mass loss towards the low-temperature regime, suggesting the addition of EVO enables the composites to be susceptible to thermal degradation. The presence of EVO makes the composites more flexible due to the fatty acids content in vegetable oil consisting of 14–22 carbon single bonds and up to three carbon double bonds per fatty acid chain. The flexibility of vegetable oil the mobility of the molecular chain, thus possessing low thermal stability. However, vegetable oils with a higher degree of carbon double and triple bonds can improve the mechanical and thermal properties of composites, depending on the added amount [35, 36].

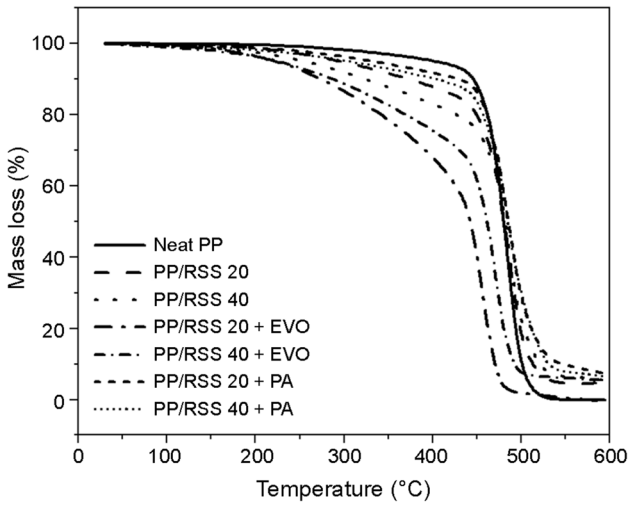

Fig. 9 TGA thermograms of PP/RSS composites without/with EVO and PA

The thermal degradation rate of PP/RSS composites with/without EVO is tabulated in Table 1. Natural-filled polymer composites are susceptible to degrade thermally due to the lignocellulose content. Without the presence of EVO and PA, the thermal degradation rate of the composites increased with RSS loading below 400 °C and has significantly reduced at T = 500–600 °C. Below 400 °C, the in-bound water and organic contents in the composite were decomposed. Increasing the temperature up to 400 °C inhibited thermal decomposition of the composites due to the formation of char that created a barrier on the composites to further decompose [37]. However, the thermal degradation rate of EVO-compatibilised composite at 400–500 °C is low (48.883%/min) for 40 php RSS compared to composites with 20 php RSS (61.5055%/min) despite having more lignocellulose content. At this temperature range, carbon–carbon chains tend to dissociate, form radicals and recombine to form a structure as reported by Bengtsson et al. [38]. Cross-linking at higher temperatures results in an improvement in

Table 1 Thermal degradation rate (%/min) of uncompatibilized, EVO and PA-compatibilized PP/RSS composites at different filler contents and temperature range

Sample	Thermal degradation rate (%/min)				
	100–200 °C	200–300 °C	300–400 °C	400–500 °C	500–600 °C
PP/RSS					
0	0	0.1020	0.6356	30.2734	68.9860
20	0.2958	1.2032	5.3215	27.4454	62.0495
40	0.6543	2.6058	9.1454	25.9401	55.5390
PP/RSS + EVO					
20	1.4371	3.2999	10.7319	61.5055	23.0256
40	1.8899	3.8387	13.7109	48.8830	31.6775
PP/RSS + PA					
20	1.7894	1.1046	5.2760	21.6404	64.5860
40	1.6206	2.2439	7.9452	24.3969	57.1534

the mechanical properties of the composites due to the formation of network structure and improvement in interfacial bonding that is consequently formed by functional groups in vegetable oil and lignocelluloses [39]. This also explains the improvement of thermal stability of EVO-compatibilized composites with a distinct reduction of thermal decomposition rate at 500–600 °C in comparison to the temperature range of 400–500 °C.

Generally, the thermal decomposition behavior of PP/RSS composites with/without PA has a similar trend as presented in Fig. 9. The degradation temperature is observed skewing towards a higher temperature regime when PA was incorporated in the system, from 500 to 540 and 550 °C at PP loading of 0, 20, and 40 php, respectively. This suggests PA has significantly enhanced the thermal stability of PP/RSS composites. Anhydrides such as PA and maleic anhydride have thermal decomposition temperature at the range of 370–490 °C [40]. Maslowski et al. used a type of anhydride in lignin-filled polymer composites and found that compatibilized composites with biofillers possessed an improved thermal decomposition temperature than neat polymer and uncompatibilized composites [41]. Similar findings were reported by Ismail et al. for PA-compatibilized LDPE/tyre dust composites [42]. A secondary bonding is known as lignin phthalate formed between the lignins in natural filler and PA, which increases the mechanical and thermal properties of the composites.

Besides improvement in interfacial adhesion between matrix and filler, high stiffness, and bulkiness of functional groups in PA increase the thermal stability of the composites by increasing the degree of crystallinity of the composites [43]. These two factors restrict the deformation and mobility of the composites at a higher temperature [32]. From Table 1, the thermal decomposition rate of PA-compatibilized composite is low at a temperature range of 100–500 °C and higher than uncompatibilized PP/RSS composites at $T > 500$ °C, suggesting PA enhanced the thermal stability of PP/RSS composites, where the decomposition of the compatibilized composites occurred at high-temperature regimes. Contrarily, the thermal decomposition rate of EVO-compatibilized composites reduced at $T > 500$ °C. Both PA and EVO responded differently to the thermal stability of PP/RSS composites mainly due to the different nature of compatibilization effect introduced in the system, where PA predominantly affected the secondary bonding between RSS and EVO improved the mobility of the polymer chain. In PA-compatibilized composites, the thermal stability is mainly caused by the presence of acrylic anhydride (RCO–O–COR) with C=O [44]. Pang et al. reported that the incorporation of PA in a natural fiber-based composite resulted in a formation of a monoester compound with a pendant carboxylic group, and this was confirmed by a FTIR spectrum [45]. Meanwhile in EVO-compatibilized composites, the hydrogen bonding forms between hydroxyl moieties of RSS and the oxygen of oxirane in EVO. The oxirane oxygen content is controlled by the epoxy sites to form interactions between RSS-EVO, which also consequences the plasticizing effect of the composites [46].

The effect of EVO and PA on water absorption properties of PP/RSS composites

The water absorption of the composites with/without the compatibilizers are presented in Fig. 10. Figure 10a depicts the water absorption rate of PP/RSS with/without EVO and Fig. 10b with/without PA. The overall trends are similar but EVO-compatibilized systems at RSS loadings > 20 php recorded a rapid increase in water uptake for the first seven days and the value was eventually plateaued-off after 15 days of water immersion. The same trend was observed only in PA-compatibilized composites only at 40 php of RSS, where

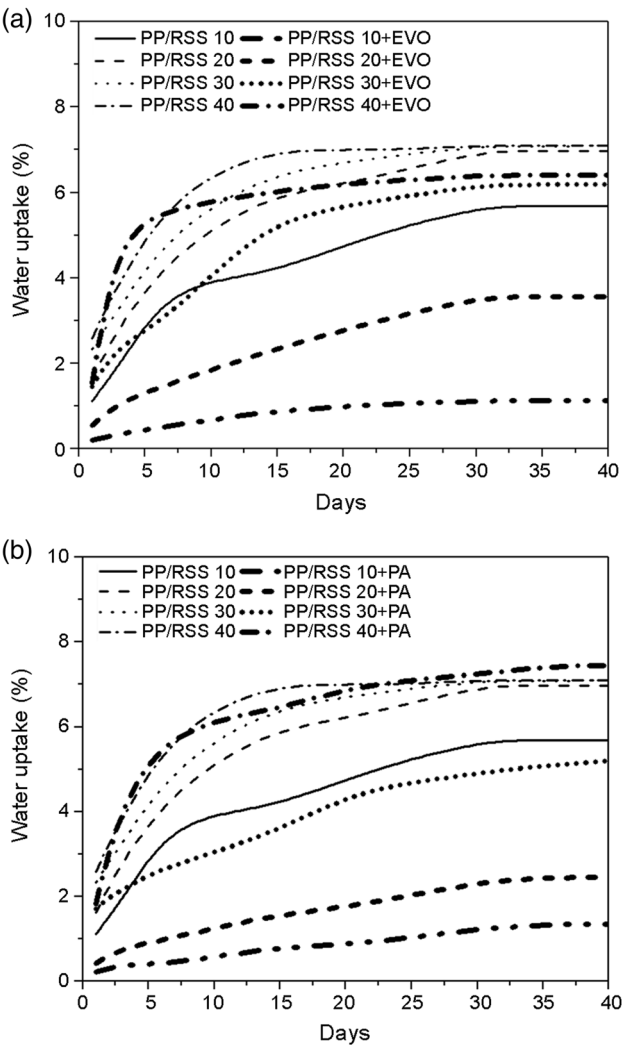

Fig. 10 Water uptake of PP/RSS composites with: **a** EVO and **b** PA

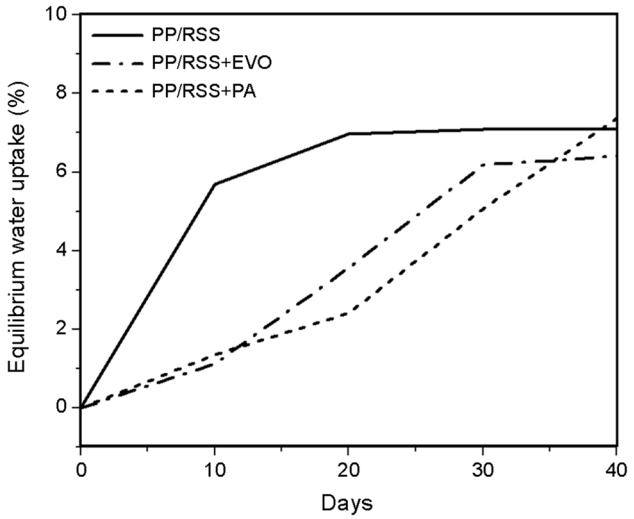

Fig. 11 Equilibrium water uptake of PP/RSS composites with EVO and PA

the water absorption percentage for both uncompatibilized and PA-compatibilized PP composites are vaguely similar at this RSS concentration. We postulate that the concentration of EVO is unable to counter the available hydrophilic RSS sites in the composites at 40 php to inhibit water uptake. The esterification reaction of the anhydrides in PA with hydroxyl groups of RSS improved the compatibility thus restricting the water molecules to penetrate the composites [47].

PP/RSS composites with EVO absorbed much lesser water even at all RSS concentrations compared to the uncompatibilized systems. Vegetable oils are commonly used in natural resources to restrict water absorption due to the enormous water retention ability in natural resources [48]. Epoxidization of vegetable oils enables the bonding between acidic sites in oil with the active water absorbance sites in natural resources [49]. This process further restricts the water absorption in natural-filled composites, as it has occurred with RSS of the present work.

Figure 11 shows the equilibrium water uptake for PP/RSS composites with PA and EVO at varied RSS loading. Equilibrium water uptake is obtained from the water absorption plot when the percentage of water uptake observed no changes for a period of time. For uncompatibilized composites, below 20 php, the equilibrium water uptake increases rapidly, and the value plateaued off when RSS was added more than 20 php. At a low concentration regime, below 20 php in our work, the water molecules being absorbed onto the hydrophilic sites of cellulose in RSS and the absorption is saturated beyond 20 php of RSS. The incorporation of EVO steadily increases the equilibrium water uptake with RSS loading with a plateau region observed at RSS loading > 30 php. For PA-compatibilized composites, the trend for equilibrium water uptake witnessed a break-point at RSS loading = 20 php. Below 20 php, the water uptake increases gradually, and a steeper slope observed when RSS loading > 20 php. The steady and gradual trends of the equilibrium water uptake of EVO and PA- compatibilized PP/RSS are predominantly caused by the enhancement of interfacial matrix-filler interactions and adhesions [30, 43]. At RSS > 30 php regime, the EVO-compatilized system has the lowest equilibrium water uptake compared to uncompatibilized and PA-compatibilized composites. This suggests that the epoxidized oil manage to seal-off the active hydrophilic sites of RSS effectively, inhibiting the permeation of water molecules into the composite system.

Conclusion

The mechanical, thermal, and water absorption properties of RSS-filled composites largely depend on RSS concentration. The tensile, flexural, and impact properties of the composites depreciated with RSS concentration and improved with the addition of EVO and PA. At high loadings, RSS has more tendency to form agglomerations due to strong interfiller interactions. The basis of interactions between filler particles is pivoted to the chemical substituents that exist in the structure. This created high heterogeneity between the matrix and filler. In composite systems with EVO, the matrix–RSS interactions were strengthened through the epoxide reactive sites. For the PA-contained systems, the mechanical properties of PP/RSS composites were enhanced mainly due to the stiffness and bulkiness of PA and ester linkages formed between anhydrides and hydroxyl groups in RSS. The chain mobility of the composites was restricted hence resulted in the weakening of EB values. EVO-compatibilized composites possessed lower thermal stability compared to the PA-compatibilized composites. This is predominantly caused by the chain flexibility introduced by an oil-based compatibilizer. PA-compatibilized composites recorded a better resistance to water absorption due to the enhanced matrix-filler interactions, which perturbed the water molecules to access the hydrophilic sites in RSS. In short, RSS can substitute conventional and costly natural and synthetic fillers to produce sustainable polymer composites with acceptable mechanical and thermal properties.

References

1. Panda AK, Singh RK, Mishra SK (2010) Thermolysis of waste plastics to liquid fuel: a suitable method for plastic waste management and manufacture of value-added products—a world prospective. Renew Sust Energ Rev 14:233–248
2. Jambeck JK, Geyer R, Wilcox C, Siegler TR, Perryman M, Andrady A, Law KL (2015) Plastic waste inputs from land into the ocean. Science 47:768–771

3. Rigamonti L, Grosso M, Møller J, Sanchez VM, Magnani S, Christensen TH (2014) Environmental evaluation of plastic waste management scenarios. Resour Conserv Rec 85:42–53
4. Kim JT, Netravali AN (2010) Mercerization of sisal fibers: effect of tension on mechanical properties of sisal fiber and fiber-reinforced composites. Compos Part A Appl Sci Manuf 41:1245–1252
5. Xu Y, Wang RH, Koutinas AA, Webb C (2010) Microbial biodegradable plastic production from a wheat-based biorefining strategy. Process Biochem 45:153–163
6. Whistler RL, Daniel JR (2000) Starch Kirk-othmerencyclopedia of chemical technology. Wiley, New York
7. Lund D, Lorenz KJ (1984) Influence of time, temperature, moisture, ingredients, and processing conditions on starch gelatinization. Crit Rev Food Sci Nutr 20:249–273
8. Zaaba NF, Ismail H (2019) Thermoplastic/natural filler composites: a short review. J Phys Sci 30:81–99
9. Ling PA, Ismail H (2013) Tensile properties, water uptake, and thermal properties of polypropylene/waste pulverized tire/kenaf (PP/WPT/KNF) composites. BioResources 8:806–817
10. Spiridon I (2014) Natural fiber-polyolefin composites. Mini Rev Cell Chem Technol 48:599–611
11. Sain M, Suhara P, Law S, Bouilloux A (2005) Interface modification and mechanical properties of natural fiber-polyolefin composite products. J Reinf Plast Compos 24:121–130
12. Oluodo LA, Huda N, Komilus CF (2018) Potential utilization of rubber seed meal as feed and food. Int J Eng 7:64–71
13. Ekebafe LO, Imanah JE, Ekebafe MO, Ugbesia SO (2010) Graft polymerization of polyacrylonitrile onto rubber (*Hevea brasiliensis*) seed shell-cellulosic and its utilization potential for heavy metal uptake from aqueous medium. Pac J Sci Technol 11:488–498
14. Malkapuram R, Kumar V, Negi YS (2009) Recent development in natural fiber reinforced polypropylene composites. J Reinf Plast Compos 28:1169–1189
15. Naveen R, Rakeshkumar C, Sanjana L, Shwetha C, Vignesh S (2020) Moisture absorption studies on Kenaf composites at various temperatures. IOP Conf Ser Mater Sci Eng 764:012016
16. Surya I, Kudori SNI, Ismail H (2019) Effect of partial replacement of kenaf by empty fruit bunch (EFB) on the properties of natural rubber latex foam (NRLF). BioResources 14:9375–9391
17. Tan SG, Chow WS (2010) Biobased epoxidized vegetable oils and its greener epoxy blends: a review. Polym Plast Technol 49:1581–1590
18. Ismail H, Shafiq MD (2014) The comparison of properties of (rubber tree seed shell flour)-filled polypropylene and high-density polyethylene composites. J Vinyl Addit Technol 22:91–99
19. Ozkoc G, Bayram G, Bayramli E (2005) Short glass fiber reinforced ABS and ABS/PA6 composites: processing and characterization. Polym Compos 26:745–755
20. Huang HX, Zhang JJ (2009) Effects of filler–filler and polymer–filler interactions on rheological and mechanical properties of HDPE–wood composites. J Appl Polym Sci 111:2806–2812
21. Ismail H, Edyham MR, Wirjosentono B (2002) Bamboo fibre filled natural rubber composites: the effects of filler loading and bonding agent. Polym Test 21:139–144
22. Samal S (2020) Effect of shape and size of filler particle on the aggregation and sedimentation behavior of the polymer composite. Powder Technol 366:43–51
23. Ananthapadmanabha GS, Deshpande V (2018) Influence of aspect ratio of fillers on the properties of acrylonitrile butadiene styrene composites. J Appl Polym Sci 135:46023
24. Silverajah VS, Ibrahim NA, Yunus WMZW, Hassan HA, Woei CB (2012) A comparative study on the mechanical, thermal and morphological characterization of poly(lactic acid)/epoxidized palm oil blend. Int J Mol Sci 13:5878–5989
25. Lee JT, Kim MW, Song YS, Kang TL, Youn JR (2010) Mechanical properties of denim fabric reinforced poly (lactic acid). Fiber Polym 11:60–66
26. Charles EW, Charles AD, James WS, Mark TB (2005) PVC handbook. Hanser Publications, Ohio
27. Stark NM, Rowlands RE (2003) Effects of wood fiber characteristics on mechanical properties of wood/polypropylene composites. Wood Fiber Sci 35:167–174
28. Mustafa WA, Zainal M, Santiagoo R, Ghani AA, Othman NS, Affandi RD (2018) Structure analysis on polypropylene maleic anhydride (PPMAH)/polypropylene (PP)/recycled acrylonitrile butadiene rubber (NBRr)/banana skin powder (BSP) composites treatment. J Adv Res Fluid Mech Therm Sci 50:40–46
29. Ragunathan S, Mustaffa Z, Kamarudin H, Sam ST, Ismail H (2017) The effect of polypropylene maleic anhydride on polypropylene/(recycled acrylonitrile butadiene rubber)/(sugarcane bagasse) composite. J Vinyl Addit Technol 23:228–233
30. Osman H, Ismail H, Mustapha M (2010) Effects of maleic anhydride polypropylene on tensile, water absorption, and morphological properties of recycled newspaper filled polypropylene/natural rubber composites. J Compos Mater 44:1477–1491
31. Amin A, Darweesh HHM, Morsi SMM, Ayoub MMH (2011) Effect of phthalic anhydride-based hyperbranched polyesteramide on cement characteristics. J Appl Polym Sci 120:3054–3064
32. Demir H, Atikler U, Balköse D, Tıhmınlıoğlu F (2006) The effect of fiber surface treatments on the tensile and water sorption properties of polypropylene–luffa fiber composites. Compos Part A Appl Sci Manuf 37:447–456
33. Samarth NB, Mahanwar PA (2015) Modified vegetable oil-based additives as a future polymeric material—review. Open J Org Polym Mater 5:1–22
34. Brostow W, Lobland HEH (2010) Brittleness of materials: implications for composites and a relation to impact strength. J Mater Sci 45:242–250
35. Manthey NW, Cardona F, Aravinthan T, Wang H, Cooney T (2010) Natural fibre composites with epoxidized vegetable oil (EVO) resins: a review. Proc South Region Eng Conf (SREC 2010) 100–107
36. Zhang C, Garrison TF, Madbouly SA, Kessler MR (2017) Recent advances in vegetable oil-based polymers and their composites. Prog Polym Sci 71:91–143
37. Zakaria Z, Ishak MM, Abdullah M, Ismail K (2010) Rice husk char and their blends during pyrolysis and combustion via thermogravimetric analysis. Int J Chem Technol 2:78–87
38. Bengtsson M, Oksman K (2006) Silane crosslinked wood plastic composites: processing and properties. Compos Sci Technol 66:2177–2186
39. Liu W, Qiu J, Zhu L, Fei ME, Qiu R, Sakai E, Tang G (2018) Tannic acid-induced crosslinking of epoxidized soybean oil for toughening poly(lactic acid) via dynamic vulcanization. Polymer 148:109–118
40. Hwang SW, Lee SB, Lee CK, Lee JY, Shim JK, Selke SE, Auras R (2012) Grafting of maleic anhydride on poly(L-lactic acid). Effects on physical and mechanical properties. Polym Test 31:333–344
41. Masłowski M, Miedzianowska J, Strzelec K (2018) Natural rubber composites filled with cereals straw modified with acetic and maleic anhydride: preparation and properties. J Polym Environ 26:4141–4157
42. Ghani SA, Feng YZ, Ismail H (2012) Properties of tyre dust-filled low-density polyethylene composites: the effect of phthalic anhydride. Polym Plast Technol Eng 51:358–363
43. Zhu Y, Liang C, Bo Y, Xu S (2015) Compatibilization of polypropylene/recycled polyethylene terephthalate blends with maleic anhydride grafted polypropylene in the presence of diallyl phthalate. J Polym Res 22:35–47

44. Hanif MPM, Supri AG, Zainuddin F (2015) Effect of phthalic anhydride on tensile properties and thermal stability of recycled high-density polyethylene/wood fiber composites. J Teknol 74:1–7
45. Pang AL, Ismail H (2014) Studies on the properties of polypropylene/(waste tire dust)/kenaf (PP/WTD/KNF) composites with addition of phthalic anhydride (PA) as a function of KNF loading. J Vinyl Addit 20:193–200
46. Chieng BW, Ibrahim NA, Then YY, Loo YY (2014) Epoxidized vegetable oils plasticized poly(lactic acid) biocomposites: mechanical, thermal and morphology properties. Molecules 19:16024–16038
47. Mishra S, Naik JB (1998) Absorption of steam and water at ambient temperature in wood polymer composites prepared from agro-waste and Novolac. J Appl Polym Sci 68:1417–1421
48. Demirel GK, Temiz A, Jebrane M, Terziev N, Gezer ED (2018) Micro-distribution, water absorption, and dimensional stability of wood treated with epoxidized plant oils. BioResources 13:5124–5138
49. Demirel GK, Temiz A, Demirel S, Jebrane M, Terziev N, Gezer ED, Ertas M (2016) Dimensional stability and mechanical properties of epoxidized vegetable oils as wood preservatives. Eur Cooperation Sci Technol 49–5